

# Cobalt–nickel composite films synthesized by chemical bath deposition method as an electrode material for supercapacitors

Sunil G. Kandalkar · Hae-Min Lee ·  
Seung Hye Seo · Kangtaek Lee · Chang-Koo Kim

Received: 29 July 2010 / Accepted: 8 December 2010 / Published online: 21 December 2010  
© Springer Science+Business Media, LLC 2010

**Abstract** Cobalt–nickel (Co–Ni) composite thin films were fabricated on copper substrates using a simple chemical bath deposition route in an ammonia-complexed solution containing cobalt chloride and nickel chloride. The structural and morphological properties of the film confirmed that the chemically deposited Co–Ni composites formed in the hydroxide phase and were well covered with irregular shaped nano-platelets. The chemically deposited Co–Ni composite electrode exhibited a maximum specific capacitance of 324 F/g, which was much larger than that of the pristine components. The cyclic voltammetry and charge–discharge test showed that the capacitance of the chemically deposited Co–Ni composite electrode mainly consisted of a pseudocapacitance.

## Introduction

Electrochemical capacitors are potentially promising energy storage devices. Supercapacitors can pack an energy that is up to 100 times larger than conventional capacitors, and can also deliver a power that is ten times higher ordinary batteries [1]. Two types of electrochemical capacitors exist based on an electrochemical response. The most commonly known capacitors are called electrical double-layer capacitors (EDLCs), which exhibit a high

surface reactivity, resulting in the formation of a double layer. The second category of capacitor materials have Faradaic electrochemical reactions occurring on the surface. Consequently, these classes of capacitors are called pseudocapacitors. The EDLC stores energy in the same way as a traditional capacitor through a charge separation. However, supercapacitors can store substantially more energy than conventional capacitors.

The performance of supercapacitors strongly depends on the electrode materials. Three types of electrode materials, including carbon [2, 3], conducting polymers [4, 5], and transition metal oxides [6–11], have been considered. In general, both the stability and the conductivity of the activated high surface area carbon decrease with increasing surface area [2]. Relatively, high energy and power densities have been reported for conducting polymer electrodes [3]. However, electroactive polymers can swell and shrink, which may lead to degradation during cycling. Recently, transition metal oxides have been prepared in the form of thin films and applied in supercapacitors. Several attempts were undertaken to maintain the advantages of the material properties and the several oxidation states or structures of these metal oxides/hydroxides and their composites (e.g., Ru, Co, Ni, Mn, Sn, Co–Ni, Co–Ni–Mn, etc.) [6–15]. Metal oxides/hydroxides have been considered as the most promising materials for electrochemical capacitors because their stability and specific capacitance are higher than carbons or polymers [1].

Metal hydroxides are often layered with large inter-layer spacing [16]. Recently, the development of metal hydroxides with high specific capacitances has regenerated great interest in these materials [17, 18].  $\text{Co}(\text{OH})_2/\text{Y}$ -zeolite composites have exhibited a maximum specific capacitance of 1,492 F/g [19] while  $\text{Co}(\text{OH})_2\text{-Ni}(\text{OH})_2/\text{Y}$ -zeolite composites have exhibited a specific capacitance of 479 F/g

S. G. Kandalkar · H.-M. Lee · S. H. Seo · C.-K. Kim (✉)  
Department of Chemical Engineering and Division of Energy  
Systems Research, Ajou University, San 5 Woncheon-dong,  
Yeontong-gu, Suwon 443-749, Korea  
e-mail: changkoo@ajou.ac.kr

K. Lee  
Department of Chemical and Biomolecular Engineering,  
Yonsei University, Seoul 120-749, Korea

[18]. However, the characteristics of all of these hydroxides suffered from an asymmetric charge–discharge behavior. Hydrous nickel–cobalt oxides with a high specific capacitance of about 730 F/g were obtained using an electrochemical anodic deposition method on a graphite substrate [20]. Luo et al. investigated the long-term stability of mixed oxide electrodes after cycling. They showed that the capacitance of the MNCO electrode continuously increased over the course of 300 cycles, reaching a maximum specific capacitance of 1,260 F/g [15]. Hybrid materials incorporating EDLC and pseudocapacitor materials are believed to be the next generation of high-performance supercapacitor devices.

Moreover, metal oxide/hydroxide electrodes also exhibit a supercapacitance after annealing, even though this treatment causes a significant loss in the supercapacitance because of a decrease in the hydrous content. Hence, hydrous transition metal oxides have been proposed as promising electrode materials for supercapacitors because their specific capacitance is usually very high [20–22]. Different physical and chemical methods, such as electrodeposition, vapor-phase and solution-phase methods, can be used to synthesize composite metal oxide/hydroxide electrodes [23–25]. In this regard, a chemical bath deposition (CBD) method is an effective method for depositing metal hydroxide or oxyhydroxide with unique nanostructures and a porous morphology for supercapacitor applications.

In this work, composite hydroxides containing cobalt and nickel that were prepared through CBD were synthesized and characterized. The structural, morphological, and electrochemical properties of the cobalt–nickel hydroxide films were discussed.

## Experimental

The Co–Ni composite thin films were obtained using a CBD method that was based on heating the substrates that were vertically immersed in an alkaline bath of cobalt chloride and nickel chloride. The alkaline bath was prepared using 0.1 M of  $\text{CoCl}_2 \cdot 6\text{H}_2\text{O}$  and 0.1 M of  $\text{NiCl}_2 \cdot 6\text{H}_2\text{O}$  as the cobalt and nickel sources, respectively, along with 25% aqueous ammonia. Initially, the  $\text{Co}(\text{OH})_2$  and  $\text{Ni}(\text{OH})_2$  precipitates formed, and then they were dissolved after the further addition of aqueous ammonia. The pH of the resultant solution was 12. Copper was used as the substrate in this study. This substrate was cleaned with a detergent and chromic acid, rinsed with double-distilled water, and finally treated with ultrasonic waves for 15 min. These substrates were immersed in the bath and heated. The precipitation began when the bath reached a temperature of 338 K. During the precipitation, a heterogeneous reaction occurred, and the Co–Ni hydroxide films were

deposited on the substrate. The coated substrates were removed from the bath after 300 min, washed with distilled water and dried in hot air.

The thickness of the Co–Ni composite film was measured using the weight difference method and a sensitive microbalance. The film thickness was  $0.570 \text{ mg/cm}^2$  after 300 min. The structural and morphological analyses of the Co–Ni composite films were carried out using an X-ray diffractometer (XRD) and a scanning electron microscopy (SEM), respectively. The composition of the film was identified using energy dispersive X-ray diffraction (EDX). The electrochemical studies of the Co–Ni composite film were conducted using a potentiostat (VSP-Princeton Applied Research). The supercapacitive behavior of the films was examined using cyclic voltammetry (CV) and electrochemical impedance spectroscopy (EIS) experiments in a 2 M KOH electrolyte.

## Result and discussion

### Structure and surface morphological analyses

The structure of the Co–Ni composite thin films was characterized using X-ray diffraction in the range of  $30\text{--}80^\circ$ . Figure 1 shows the XRD pattern of the as-deposited Co–Ni hydroxide thin film on the copper substrate. Small intensity peaks were observed at  $2\theta = 32.52^\circ$ ,  $38.78^\circ$ ,  $51.49^\circ$ ,  $58.06^\circ$ , and  $69.67^\circ$ , corresponding to the (022), (002), (012), (003), and (113) planes of  $\text{Co}(\text{OH})_2$ , respectively [JCPDS card no. 089-8616]. Peaks were also observed at  $2\theta = 37.97^\circ$  and  $61.81^\circ$  for the (101) and (110) planes of  $\text{Ni}(\text{OH})_2$ , respectively [JCPDS card no. 01-1047]. The three distinct peaks at  $2\theta = 43.30^\circ$ ,  $50.43^\circ$ , and  $74.99^\circ$  represented the Cu (111), Cu (200), and Cu (220) planes, respectively [JCPDS card no. 04-0836]. The XRD

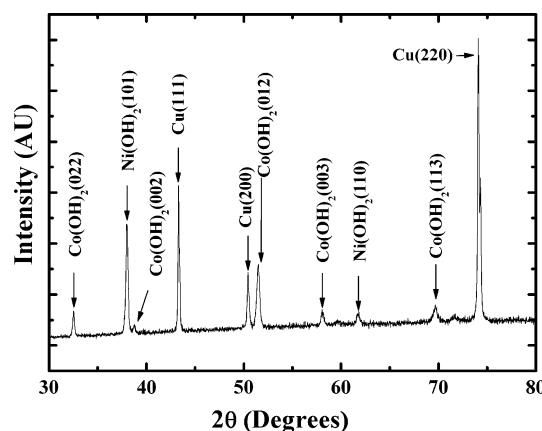


**Fig. 1** XRD pattern of the Co–Ni composite thin film chemically that was deposited on the copper substrate

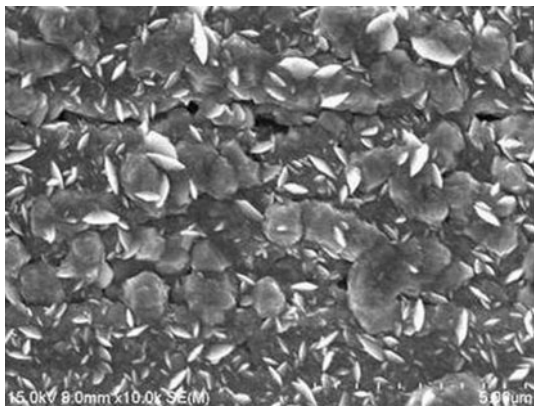


**Fig. 2** SEM image of the chemically deposited Co–Ni composite thin film

measurements revealed the formation of the Co–Ni composites in the hydroxide phase. The EDX elemental mapping was carried out in order to identify the composition of the film. From the EDX analysis, the chemical composition of the deposited film was  $\text{Co}_{0.69}\text{Ni}_{0.26}\text{O}_{0.05}$ .

Figure 2 shows the SEM image of the chemically deposited Co–Ni composite thin film. The surface of the Co–Ni composite film was compact and well covered with irregular shaped nanoplatelets that had random sizes. These platelets were randomly distributed over the whole surface of the substrate. Some cracks were observed because of the terminal thickness of the Co–Ni composite film. In addition, the Co–Ni composite film exhibited a porous morphology, which are prime requirements in supercapacitor applications.

**Supercapacitive analysis**

The chemically deposited Co–Ni composite films were employed as electrochemical supercapacitors. The supercapacitive performance of the Co–Ni composite electrode was evaluated using CV, the charge–discharge technique, and EIS measurements.

Figure 3 shows the CV curve of the Co–Ni composite electrode in the 2 M KOH electrolyte at a scan rate of 20 mV/s. The shape of the curve revealed that the capacitance characteristics of the chemically deposited Co–Ni composite electrode were distinct from the electric double-layer capacitance, which produced a CV curve that was close to an ideal rectangular shape. The results indicate a good capacitive response from the electrode. Two quasi-reversible electron transfer processes were visible in the CV curve, indicating that the capacity mainly arose from the pseudocapacitive capacitance. Since the voltammetric responses on the positive sweeps are fairly symmetrical with their counterparts on the negative sweeps, the Co–Ni composite film can be employed as an electrode material for electrochemical supercapacitors.

The capacitance ( $C$ ), the interfacial capacitance ( $C_i$ ), and the specific capacitance ( $C_s$ ) were calculated from

$$C = \frac{I}{dV/dt} \tag{1}$$

$$C_i = \frac{C}{A} \tag{2}$$

$$C_s = \frac{C}{W} \tag{3}$$

where  $I$  is the average current,  $dV/dt$  is the scanning rate,  $A$  is the area of the electrode that was dipped in the electrolyte, and  $W$  is the mass of the electrode. From Fig. 3, the chemically deposited Co–Ni composite electrode exhibited maximum specific and interfacial capacitances of 324 F/g and  $0.518 \text{ F/cm}^2$ , respectively. Deng et al. [26] reported that the specific capacitance for Co–Ni prepared by coprecipitation method was 287 F/g, which is less than the one obtained in this study. Therefore, the specific capacitance of the Co–Ni composite improved probably because of the nanoplatelets morphology of the composite.

Figure 4 shows the charge–discharge behavior of the chemically deposited Co–Ni composite electrode between  $-0.1$  and  $+0.45 \text{ V}$  at a current density of  $1 \text{ mA/cm}^2$ . The shape of the discharge curve did not correspond to the capacitance characteristics of pure double-layer capacitors, which was in agreement with the CV curve results. During the discharge period, two variation regimes were observed. The non-linear variation in the potential ( $-0.1$  to  $0 \text{ V}$ ) with respect to time indicated a typical pseudocapacitance behavior, resulting from the electrochemical redox reaction at the interface between the electrode and the electrolyte. In the other part of the discharge curve, the linear variation in the potential with time indicated an electric double-layer capacitance, which was rooted in the charge separation

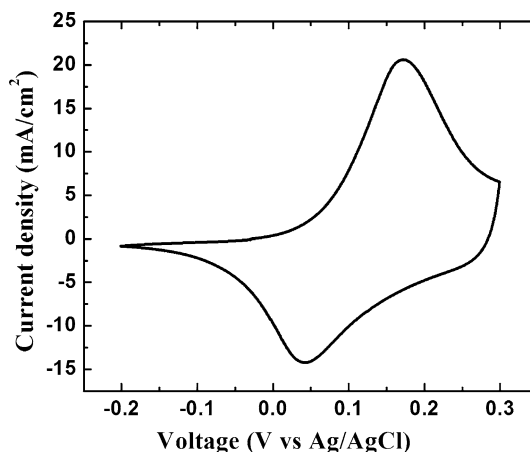


**Fig. 3** CV curve of the chemically deposited Co–Ni composite electrode in the 2 M KOH electrolyte. The scanning rate was 20 mV/s

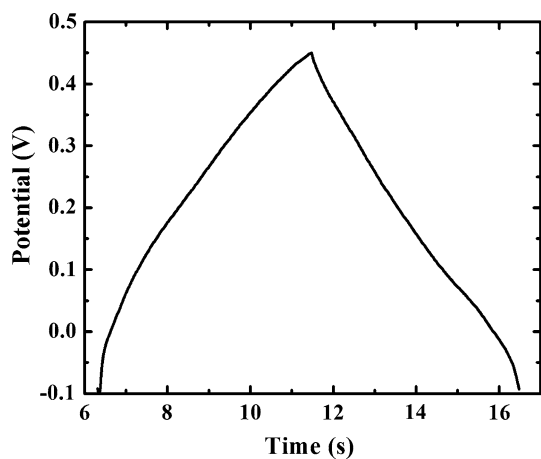


**Fig. 4** Charge–discharge curve of the chemically deposited Co–Ni composite electrode in the 2 M KOH electrolyte. The charging current was 1 mA/cm<sup>2</sup>

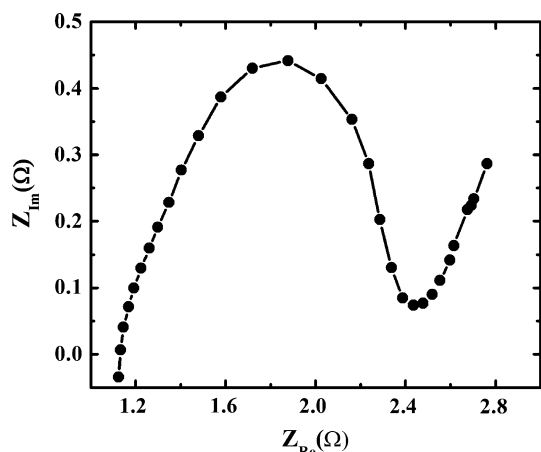


**Fig. 5** The complex-plane impedance plot of the chemically deposited Co–Ni composite electrode

across the interface between the electrode and the electrolyte.

The electrochemical impedance measurements were carried out at a potential of 0.6 V in a frequency range of  $10^{-2}$  to  $10^5$  Hz. Figure 5 shows the complex-plane impedance plot of the supercapacitor cell assembly based on the chemically deposited porous Co–Ni composite electrode. The impedance spectrum of the cell exhibited a distorted semicircle in the high frequency region while a slope line in the low frequency region. This implies that the supercapacitors exhibit a blocking behavior at high frequencies and a capacitive behavior at low frequencies. In the mid-frequency range, the cell behaved as a combination of a resistor and a capacitor, where the porosity of the electrode and the thickness of the electroactive materials played vital roles in the determination of the capacitance values.

## Conclusions

The Co–Ni composite thin films were prepared on the copper substrate using a simple CBD method. The XRD measurements confirmed that the Co–Ni composites were formed in the hydroxide phase. The SEM analysis showed that the chemically deposited Co–Ni composite was well covered with irregular shaped nanoplatelet. In addition, from the SEM images, the composite exhibited a porous morphology. The electrochemical study revealed that the chemically deposited Co–Ni composite electrode had a specific capacitance of 324 F/g. The CV and charge–discharge curves confirmed that the capacitance of the test electrode mainly consisted of a pseudocapacitance. The EIS showed that the capacitive behavior was observed in the low frequency region, whereas the resistive behavior was observed in the high frequency region. The chemically deposited Co–Ni composite electrode could potentially be applied to a simple method with a low cost and high capacitance for electrochemical capacitors.

**Acknowledgements** This work was supported by the Basic Science Research Program through the National Research Foundation of Korea (NRF) funded by the Ministry of Education, Science and Technology (Grant No. 2009-0070734) and Ajou University Research fellowship of 2007 and 2010 (Grant No. 20072650 and S-2010-G0001-00058).

## References

1. Conway BE (1999) Electrochemical supercapacitors. Kluwer/Plenum Publishers, New York
2. Kim C (2005) J Power Sources 142:382
3. Kong LB, Zhang J, An JJ, Luo YC, Kang L (2008) J Mater Sci 43:3664. doi:10.1007/s10853-008-2586-1
4. Frackowiak E, Khomeiko V, Jurewicz K, Lota K, Beguin F (2006) J Power Sources 153:413
5. Zhang J, Kong LB, Li H, Luo YC, Kang L (2010) J Mater Sci 45:1947. doi:10.1007/s10853-009-4186-0
6. Wang YG, Zhang XG (2004) Electrochim Acta 49:1957
7. Hu CC, Chen WC (2004) Electrochim Acta 49:3469
8. Srinivasan V, Weidner JW (2000) J Electrochem Soc 147:880
9. Kandalkar SG, Gunjekar JL, Lokhande CD (2008) Appl Surf Sci 254:5540
10. Nam KW, Kim KB (2002) J Electrochem Soc 149:A346
11. Cao L, Lu M, Li HL (2005) J Electrochem Soc 152:A871
12. He KX, Wu QF, Zhang XG, Wang XL (2006) J Electrochem Soc 153:A1568
13. Wu NL (2002) Mater Chem Phys 75:6
14. Fan Z, Chen J, Cui K, Sun F, Xu Y, Kuang Y (2007) Electrochim Acta 52:2959
15. Luo JM, Gao B, Zhang XG (2008) Mater Res Bull 43:1119
16. Ramesh TN, Rajamathi M, Kamath PV (2003) Solid State Sci 5:751
17. Zhao DD, Bao SJ, Zhou WJ, Li HL (2007) Electrochem Commun 9:869
18. Liang YY, Bao SJ, Li HL (2007) J Solid State Electrochem 11:571
19. Cao L, Xu F, Liang YY, Li HL (2004) Adv Mater 16:1853

20. Hu CC, Cheng CY (2002) *Electrochem Solid State Lett* 5:A43
21. Pang SC, Anderson MA, Chapman TW (2000) *J Electrochem Soc* 147:444
22. Hu CC, Chen WC, Chang KH (2004) *J Electrochem Soc* 151:A281
23. Castro EB, Real SG, Pinheiro Dick LF (2004) *Int J Hydrog Energy* 29:255
24. Jiang X, Herricks T, Xia Y (2002) *Nano Lett* 2:1333
25. Bai A, Hu CC (2005) *Electrochim Acta* 50:1335
26. Deng JJ, Deng JC, Liu ZL, Deng HR, Liu B (2009) *J Mater Sci* 44:2828. doi:[10.1007/s10853-009-3373-3](https://doi.org/10.1007/s10853-009-3373-3)